Hindawi
International Journal of Polymer Science
Volume 2022, Article ID 1196567, 13 pages
https://doi.org/10.1155/2022/1196567

Research Article

Hemispherical Molding Experiment and Simulation of Unidirectional Carbon Fiber Prepreg

Hongxiao Wang,[1,2] **Luyao Bai**,[1] **and Yanbo Hui**[1]

[1]*School of Mechanical and Electrical Engineering, Henan University of Technology, No. 100, Lianhua Street, Gaoxin District, Zhengzhou, China*
[2]*Henan Weihua Heavy Machinery Co., Ltd., No. 18 Shanhai Road, Changyuan 453400, China*

Correspondence should be addressed to Luyao Bai; 202191028@stu.haut.edu.cn

Received 24 December 2021; Accepted 15 March 2022; Published 5 April 2022

Academic Editor: Joanna Rydz

To study the deformation law and forming defects of hemispherical molding of unidirectional carbon fiber reinforced polymer (UN-CFRP), hemispherical molding experiments were carried out, and a three-dimensional finite element model of single-ply UN-CFRP hemispherical molding was established. The results show that the established finite element model can accurately predict the molding deformation law and forming defects of UN-CFRP. The results indicate that the fiber at the top of the sample is uniformly distributed; the fiber on both sides of the sample top and parallel to the fiber direction is local dispersion; the fiber at both sides of the bottom is trapezoidal splitting. The results at the bending corner show that the bending quality is better when the angle between the fiber direction and the tangent of the circular bend is in the range of 70-90°; it is easy to produce extrusion wrinkling when the angle between the fiber direction and the tangent of the circular bend is 15-70°; it is easy to produce extrusion accumulation when the angle between the fiber direction and the tangent at the circular bending is in the range of 0-15°. The results of cross-ply UN-CFRP hemispherical molding show that the full spreading property is good, and there is no obvious fold in the bending part.

1. Introduction

Nowadays, the world is facing the problems of energy constraints and environmental pollution, forcing people to find ways to achieve the light weight of aircraft, automobiles, and other travel products, to reduce fuel consumption and protect the environment. As a representative of advanced composite materials, resin-based carbon fiber reinforced composites have been widely used in aerospace, automotive, rail transportation, and other industries with their characteristics of light weight and high strength and designability, and it has become a trend to use these composites instead of metal materials for the lightweight design of aircraft and automobiles [1, 2]. However, due to the long production cycle of CFRP parts, complex production process, and lower molding speed of products than metal parts [3], it has not been able to meet the demand for high-volume and high-efficiency production in the automotive industry, so how to improve the molding efficiency of carbon fiber composites has been the focus of research by scholars at home and abroad in recent years.

The hot pressing process can rapidly manufacture various complex structures, which is the key to solving the high-volume and high-efficiency application of carbon fiber composites [4]. In the research on the composite hot pressing process, Wakeman et al. [5] used the hot pressing molding process to study the molding effect of carbon fiber woven reinforced composites with thermoplastic resin matrix in the nonisothermal molding process and found that the preheating temperature of the mold and the initial degree of resin consolidation are important factors affecting the molding quality; Alcock et al. [6] omitted the preforming process in the hot pressing process, and the results showed that this simplified process can be used to form simple composite structural parts, and it was found that temperature and pressure are the main

influencing parameters for the hot pressing of composite sheets. Gereke et al. [7] found that the compression sheet was effective in preventing the occurrence of fiber wrinkle defects in composite hot compression molding. Harrison et al. [8] showed that the spring-actuated crimping method was more effective in reducing the occurrence of wrinkle defects than the friction-actuated crimping method. Zhang et al. [9] proposed and designed a nonisothermal model for hemispherical hot stamping, explored a new hot stamping molding process for woven composite sheets directly, and achieved better molding results. Gherissi et al. [10] increased the depth of hemispherical preparation composite molding based on the study of Zhang et al. [9] and found that with the increase in molding depth, the deformation increased rapidly. There is less research literature on UN-CFRP molding research, Hongfu et al. [11] prepared a composite rectangular box for unidirectional carbon fiber composites using the rapid hot press molding technique, and the results of the study showed that precompaction has a large influence on the molding quality.

In the study of the hot pressing mechanism of composites, Bilisik [12] used the method of fiber pulling to determine the in-plane shear properties of fibers, and the results showed that different specimen aspect ratios and the number of pulled fibers had a great influence on the shear results. Charmetant et al. [13] proposed a superelastic ontology to describe the mechanical behavior of large deformations of woven glass fiber fabrics during molding. Similarly, Davey et al. [14] simulated and analyzed the semicircular stamping deformation of CF/PEEK composite sheets for different crimping forces and accurately predicted the deformation and deep-drawing properties of this material during hot compression molding. In China, Zhang et al. [15] conducted hot stretching experiments on woven composites, and the experimental results showed that the locking angle of the woven composites was 30 deg. Gong et al. [16] established a single-layer two-dimensional stamping finite element model and used it to analyze the forming of double-dome shapes of thermoplastic woven prepreg. Peng and Cao [17] also did a lot of work for the molding performance of woven composites, used the hyperelasticity principal structure to describe the principal structure equations of the complex mechanical behavior of woven composites during the molding process, and performed a multifield coupled and multiscale analysis of the hot compression molding process. Notably, Haanappel et al. [18] studied the molding quality of braided composites (CF/PPS) and unidirectional composites (CF/PEEK) by comparing them through experimental and finite element simulations using stiffened sheets, and the results showed more folds due to higher in-plane shear resistance of PEEK-based unidirectional carbon fiber composites, resulting in their molded surface quality being poor.

From the above research results, it can be found that the current research on the hot compression molding process and molding mechanism of carbon fiber composites is mainly focused on woven composites. And domestic and foreign scholars have reached a unanimous conclusion on the molding deformation mechanism of woven composites: shear deformation is the main deformation mode in the hot pressing process of woven composites [19, 20]. Compared with woven composites, UN-CFRP has poorer spreadability during molding, but UN-CFRP is more designable and can take advantage of the mechanical advantages of carbon fiber composites, and it can be processed with precise cutting for higher material utilization and better production quality stability. Therefore, it is of great practical significance to study the deformation law of UN-CFRP by molding it in depth. Based on this, a hemispherical hot pressing experimental platform was built in this paper, and molding experiments were conducted on single-layer UN-CFRP. Then, a hemispherical three-dimensional molding finite element model was established, and the deformation law and molding defects of single-layer UN-CFRP in the molding process were analyzed by using this model.

Table 1: Mechanical properties of CFRP at room temperature.

Elastic property	Value of number
Longitudinal tensile modulus, E_{11} (MPa)	137,000
Transverse tensile modulus, E_{22} (MPa)	9000
Axial tensile modulus, E_{33} (MPa)	9000
Poisson's ratio, ν_{12}	0.28
Poisson's ratio, ν_{13}	0.28
Poisson's ratio, ν_{23}	0.4
Shear modulus, G_{12} (MPa)	3780
Shear modulus, G_{13} (MPa)	6000
Shear modulus, G_{23} (MPa)	6000
Density, ρ (t/mm^3)	$1.79e-9$

2. Experimental Materials and Methods

2.1. Materials Used for Experiments. The carbon fiber used in UN-CFRP studied in this paper is T300, and the matrix material is epoxy resin with a 62% volume fraction of carbon fiber, which is purchased from Weihai Guangwei Composites Co. The mechanical properties of the material are shown in Table 1 [21].

2.2. Experimental Setup. To verify the correctness of the model, a hemispherical molding experimental platform was built in this study, and the specific experimental setup is shown in Figure 1. In the figure, a manual hydraulic press with a maximum load of 20 tons was used, which was purchased from Qingdao Zhongmai Furun Machinery Equipment Co. The hemispherical mold with a diameter of 60 mm is a heatable mold, manufactured by a five-axis machining center with a machining accuracy of IT7 and a surface roughness of Ra1.6 μm. Nine electric heating rods with a power of 100 W are used to heat the hemispherical convex mold, concave mold, and platen at the same time, and the heating temperature range is from room temperature to 300°C. The temperature control equipment uses the digital display intelligent temperature electronic thermostat produced by Taizhou Hanshi Electric Heating Electric Co.

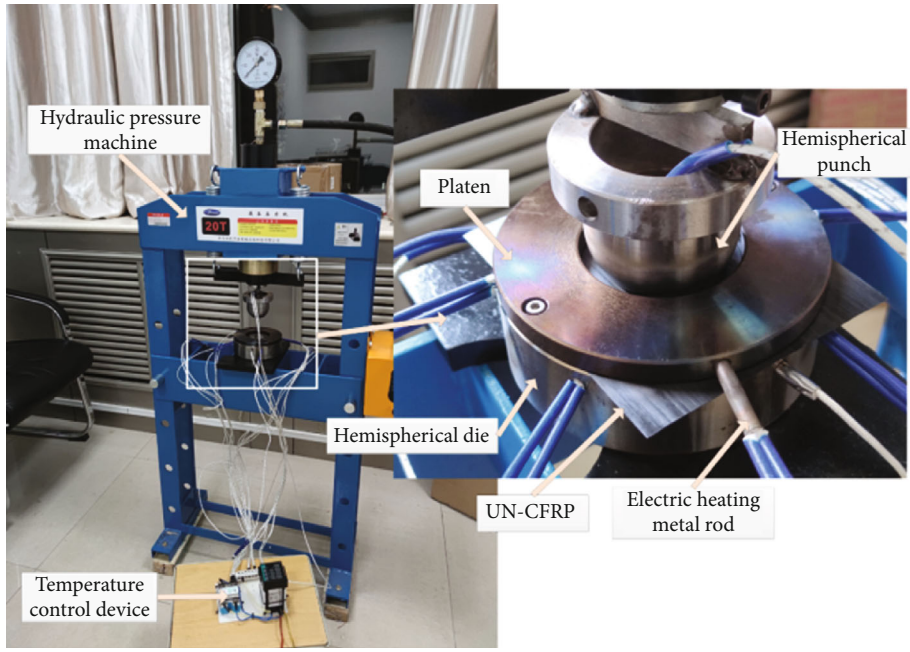

Figure 1: Hemispherical molding for UN-CFRP.

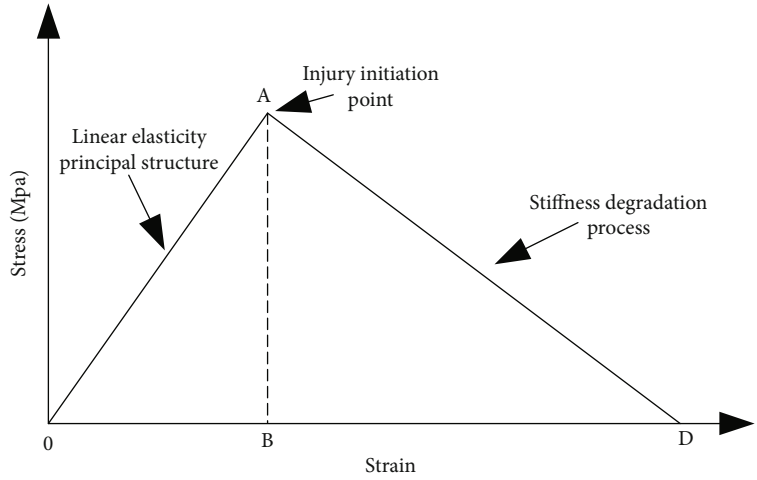

Figure 2: Carbon fiber phase damage failure model.

2.3. Experimental Procedure. To ensure that the resin would not stick to the mold during the UN-CFRP molding process and to facilitate the release of the molded parts after molding, the mold was firstly coated with a mold release agent on the convex and concave molds before the experiment, and then, the mold was preheated to 80°C for heat preservation, as the resin matrix for the experiment had the lowest viscosity at that temperature. The single-layer UN-CFRP with the size of **130** $\times$ **130** $\times$ **0.13** mm and the double-layer UN-CFRP with the layup method of [0/90] were put into the mold, respectively, and the prepreg tape was crimped using the platen, and the mold was manually closed under the loading of the press, and when the mold was completely closed, the temperature was increased to 135°C and insulated for 90 minutes, and then, natural cooling was carried out, and the mold was divided after cooling, and the parts complete the whole experimental process.

3. Finite Element Simulation of UN-CFRP Hemispherical Molding

3.1. Material Ontology Model. CFRP is defined as each anisotropic linear elastic instantiation, and the failure criterion is adopted as the three-dimensional Hashin failure criterion. The failure criterion is as follows.

Fiber longitudinal stretching:

$$F_{\text{ft}} = \left(\frac{\sigma_{11}}{X_C}\right)^2 + \alpha\left(\frac{\sigma_{12}^2 + \sigma_{13}^2}{S_L^2}\right) = 1, \quad \sigma_{11} \geq 0 \tag{1}$$

Fiber longitudinal compression:

$$F_{fc} = \left(\frac{\sigma_{11}}{X_C}\right)^2 = 1, \quad \sigma_{11} < 0 \tag{2}$$

Substrate transverse stretching:

$$F_{mt} = \left(\frac{\sigma_{22} + \sigma_{33}}{Y_c}\right)^2 + \frac{\sigma_{23}^2 + \sigma_{22}\sigma_{23}}{S_T^2} + \frac{\sigma_{12}^2 + \sigma_{13}^2}{S_L^2} = 1, \quad \sigma_{22} \geq 0 \tag{3}$$

Substrate transverse compression:

$$F_{mc} = \left[\left(\frac{Y_c}{2S_T}\right)^2 - 1\right]\left(\frac{\sigma_{22} + \sigma_{33}}{Y_c}\right) + \left(\frac{\sigma_{22} + \sigma_{33}}{2S_T}\right)^2 + \frac{\sigma_{23}^2 - \sigma_{22}\sigma_{23}}{S_T^2} + \frac{\sigma_{12}^2 + \sigma_{13}^2}{S_L^2} = 1 \tag{4}$$

In the above equations, F_{ft}, F_{fc}, F_{mt}, and F_{mc} correspond to the damage criterion of the respective damage failure mode; when the damage criterion reaches 1, the corresponding fiber failure mode starts to occur. In the experimental process, when the CFRP damage occurs after, continued processing will be accompanied by the damage evolution process, corresponding to the finite element analysis of the damage evolution process which can be characterized by unit stiffness degradation (Figure 2).

Where $0 - A$ is the initial stiffness, when stress reaches the A point that a failure criterion is greater than 1, the initial damage occurs stiffness which begins to decay. A-D is the damage evolution path; the stiffness unit at this stage begins to degrade; when the stiffness decays to the D point, the unit is removed. The damage evolution is calculated using the model of energy loss:

$$\sigma = c(d)\colon s, \tag{5}$$

where $c(d)$ is the stiffness matrix after decay, calculated by the following equation, where $D = 1 - (1 - d_f)(1 - d_m)\nu_{12}\nu_{21}$; d_f, d_m, d_s are damage variables characterizing fiber, matrix, and shear failure, respectively, and can be derived from the damage variables of the four criteria:

$$c(d) = \frac{1}{D}\begin{bmatrix} (1-d_f)E_1 & (1-d_f)(1-d_m)\nu_{12}E_1 & 0 \\ (1-d_f)(1-d_m)\nu_{12}E_2 & (1-d_m)E_2 & 0 \\ 0 & 0 & D(1-d_s)G \end{bmatrix}, \tag{6}$$

$$d_f = \begin{cases} d_f^t, & \text{if } \sigma_{11} \geq 0, \\ d_f^c, & \text{if } \sigma_{11} < 0, \end{cases} \tag{7}$$

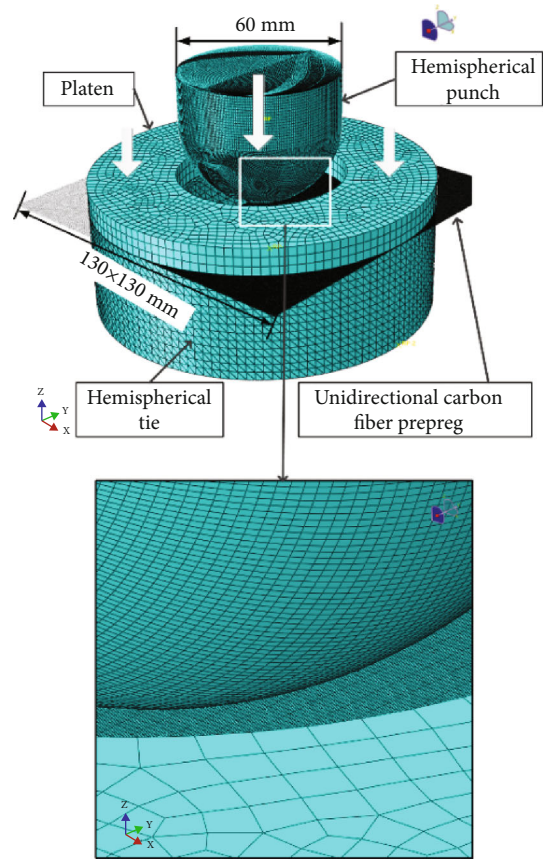

Figure 3: Finite element model of hemispherical molding for single-ply UN-CFRP.

$$d_m = \begin{cases} d_m^t, & \text{if } \sigma_{22} \geq 0, \\ d_m^c, & \text{if } \sigma_{22} < 0, \end{cases} \tag{8}$$

$$d_s = 1 - (1 - d_{\text{ft}})(1 - d_{fc})(1 - d_{mt})(1 - d_{mc}). \tag{9}$$

Abaqus comes with a damage criterion that does not have a three-dimensional Hashin failure criterion, and the calculation is performed using the FORTRAN language to write the three-dimensional Hashin failure criterion and damage evolution as a user material subroutine, VUMAT, for analytical calculations.

3.2. Finite Element Model. The model construction of the mold structure was carried out using Solidworks, and the size of the model was built according to the actual experimental size (Figure 3). The material of the convex die, concave die, and platen is 45 gauge steel with an elastic modulus of 210,000 MPa and Poisson's ratio of 0.21. Since the resin matrix is in a fluid state during UN-CFRP hot pressing, the stiffness of the mold is much higher than the stiffness of the molded material. Therefore, the hemispherical convex mold, hemispherical concave mold, and platen are defined as rigid elements, with element type R3D10, mesh size 2, and the total travel of the convex mold is 30 mm. The hemispherical concave die is meshed with tetrahedral solid elements, with a total of 103,838 elements.

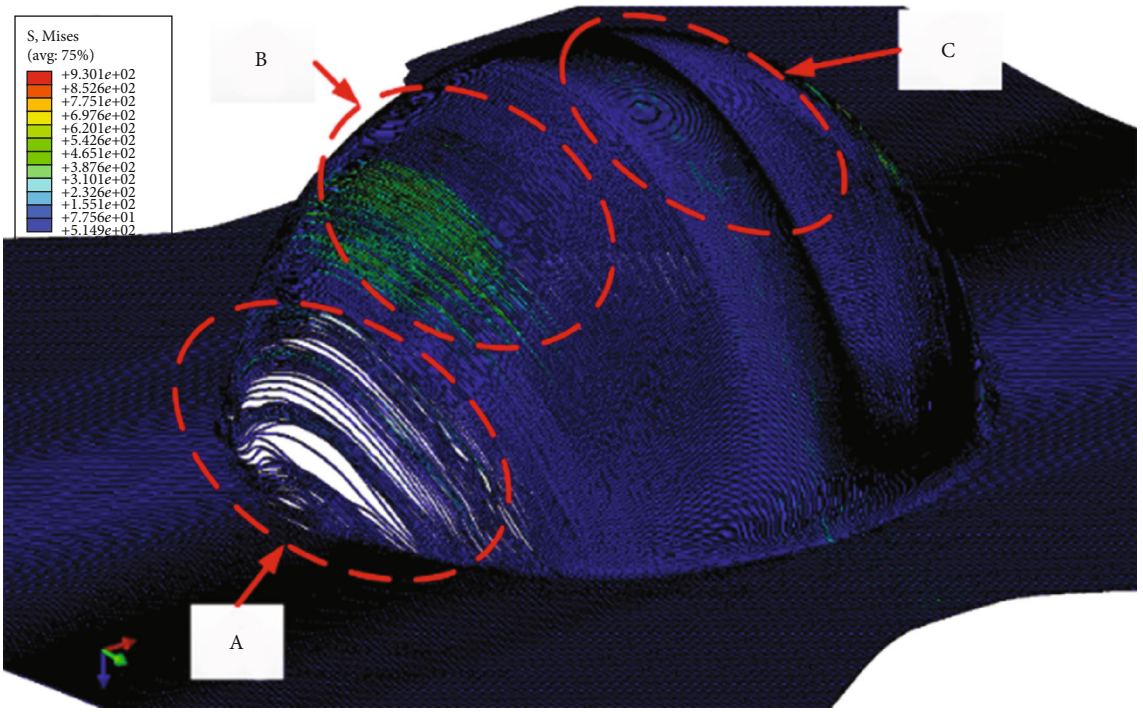

(a) Oblique view of simulation results

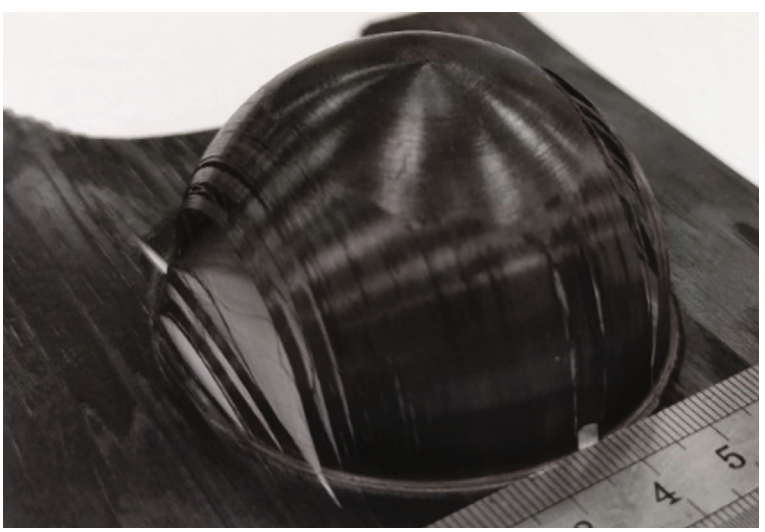

(b) Oblique view of experiment results

Figure 4: Continued.

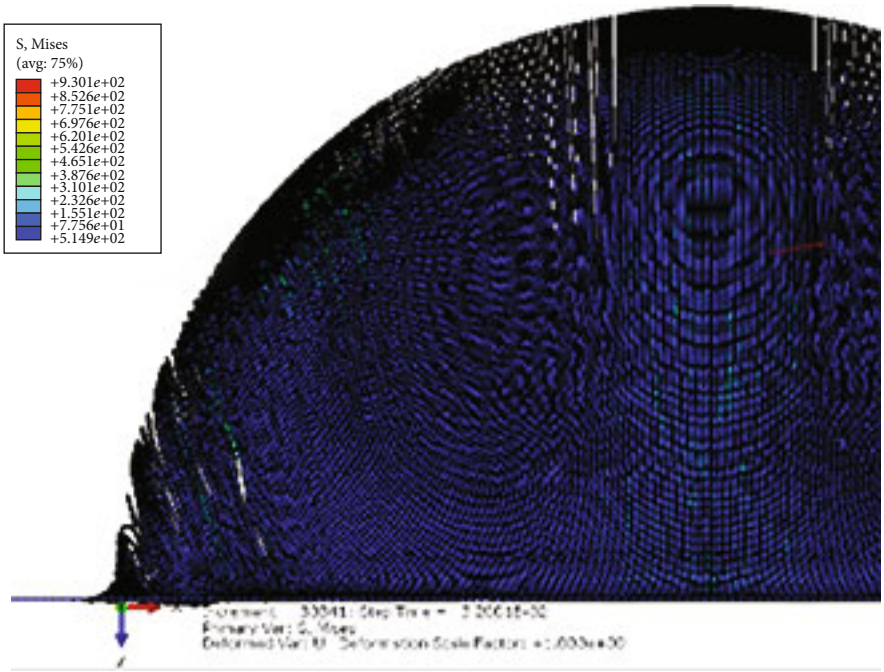

(c) Vertical view of simulation results

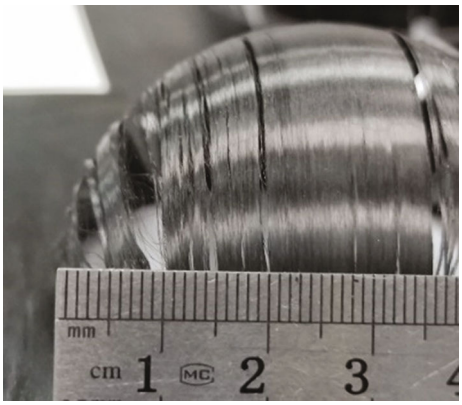

(d) Vertical view of experiment results

Figure 4: Continued.

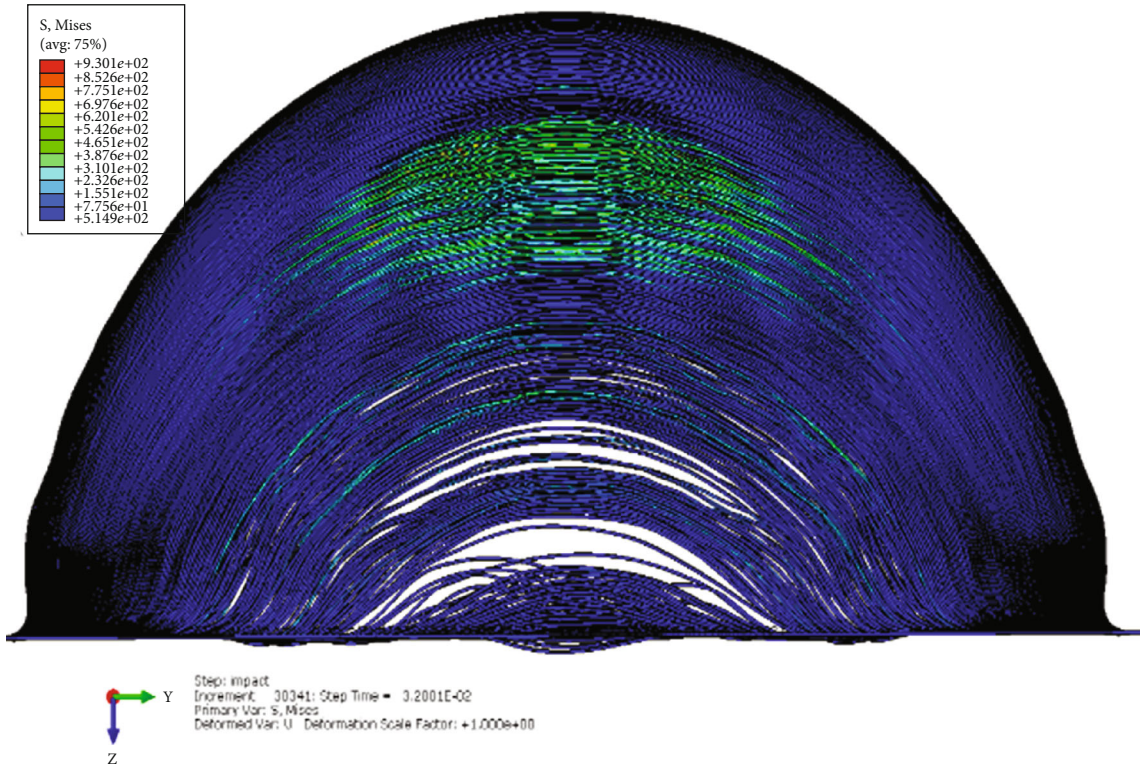

(e) Left view of simulation results

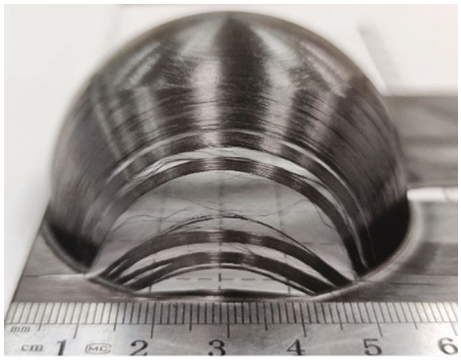

(f) Left view of experiment results

Figure 4: Comparison of finite element simulation results and experimental results from different perspectives.

Since UN-CFRP is composed of carbon fibers arranged in parallel with the same orientation, it is inevitable that the fibers will tear along the vertical fiber direction during the molding process in the hemispherical mold. If we want to characterize this tearing effect accurately, we need to model each carbon fiber, but the diameter of a single carbon fiber is between 4 and 8 microns, and the model data volume will be very large if we model it as a single carbon fiber, which makes it impossible to calculate. In this study, it was observed experimentally that due to the viscosity of the resin, the carbon fiber prepreg tape does not disperse as a single carbon fiber unit in hemispherical molding experiments, and the maximum width of its dispersion is often larger than the thickness of the single layer of prepreg tape. Therefore, in this study, it is modeled with its single-ply thickness as the minimum unit. Specifically, UN-CFRP with a thickness of 0.13 mm and a size of 130 × 130 mm is divided into rectangular long strips with a cross-section of 0.13 × 0.13 mm along the vertical fiber direction. UN-CFRP is set as an anisotropic material, and the fiber direction is along the rectangular long strip. UN-CFRP uses a three-dimensional variable elastomer, and the deformation of the specimen is mainly studied, so the specimen unit type is solid unit C3D8R and reduction integral is used. UN-CFRP is meshed with hexahedral solid elements, with a total of 2,000,000 elements.

3.3. Material Properties. Since carbon fiber itself has good heat resistance, the temperature study range in this paper is low (below 150°C), and the mechanical properties of carbon fiber basically will not change in this temperature range, so it is assumed that the mechanical properties of carbon fiber do not change with temperature in the finite

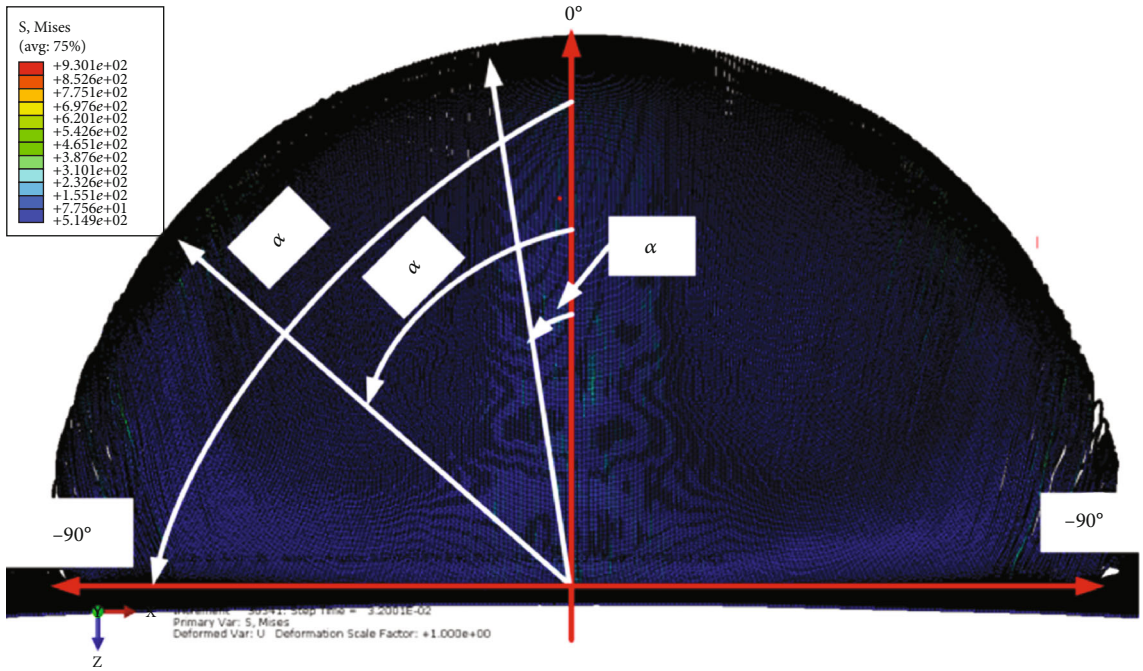

Figure 5: Circular coordinate system.

element modeling. The resin in the carbon fiber prepreg tape is epoxy resin, and the viscosity of this resin system reaches the lowest at 80°C. The best temperature for the resin to cross-link is about 135°C, so the experiment is conducted at 135°C.

3.4. Boundary Condition Setting. The Abaqus dynamic display analysis method was used to set the mold compression load of the hemispherical convex mold by displacement loading, setting the loading displacement to 30 mm, setting the uniform pressure on the surface of the platen with a size of 100 N, and setting the concave mold as a solid support constraint.

Since the friction coefficient between die and fiber and between fiber and fiber is affected by many factors such as molding speed, fiber direction, and molding temperature in the actual experimental process, the problem of setting the material contact properties in the molding process has been a difficult point in the simulation process. Since the focus of this research is on the deformation law and molding defects of UN-CFRP in the molding process, the model in setting the friction coefficient was not experimented separately in the model, and the setting method of the friction coefficient in the literature was referred to. The contact relationship between the concave and convex die, the platen, and the molding embryo is defined by means of contact pairs, and the friction coefficients between the hemispherical convex die and UN-CFRP, between the hemispherical concave die and UN-CFRP, between the platen and UN-CFRP, between the platen and the convex die, and between the carbon fiber and the carbon fiber prepreg tape are set to 0.2.

4. Result Analysis

4.1. Comparison of Experimental and Simulation Results of Single-Layer UN-CFRP. Figure 4 shows the comparison between the finite element simulation results of UN-CFRP hemispherical molding and the experimental results in different views, from which it can be seen that the simulation results are in good agreement with the experimental results. From the oblique view Figures 4(a) and 4(b), it can be seen that the hemispherical UN-CFRP has serious fiber splitting in the A area (both sides of the bottom of the specimen in parallel fiber direction) during the molding process, and from the left view Figures 4(e) and 4(f), it can be clearly seen that the fiber is splitting in a gradient, and the splitting amplitude is large, and the molding quality is poor. The fibers in zone C (the top of the specimen in parallel fiber direction) are tightly arranged, and the molding quality is good (Figures 4(c) and 4(d)).

In order to determine the range of A, B, and C zones, this study takes the center of the largest semicircular tangent in the vertical fiber direction as the coordinate origin and establishes the circular angle coordinate system shown in Figure 5. By measuring the six sample deformation areas, it can be obtained that the A zone is generally located on both sides of the specimen in the parallel fiber direction and the molded direction at ±45-90°, the B zone is generally located on both sides of the specimen in the parallel fiber direction and the molded direction at ±15-45°, and the C zone is generally located in the parallel fiber direction with ±0-15° on both sides of the top. The maximum cleavage position is located at ±45-60° in zone A.

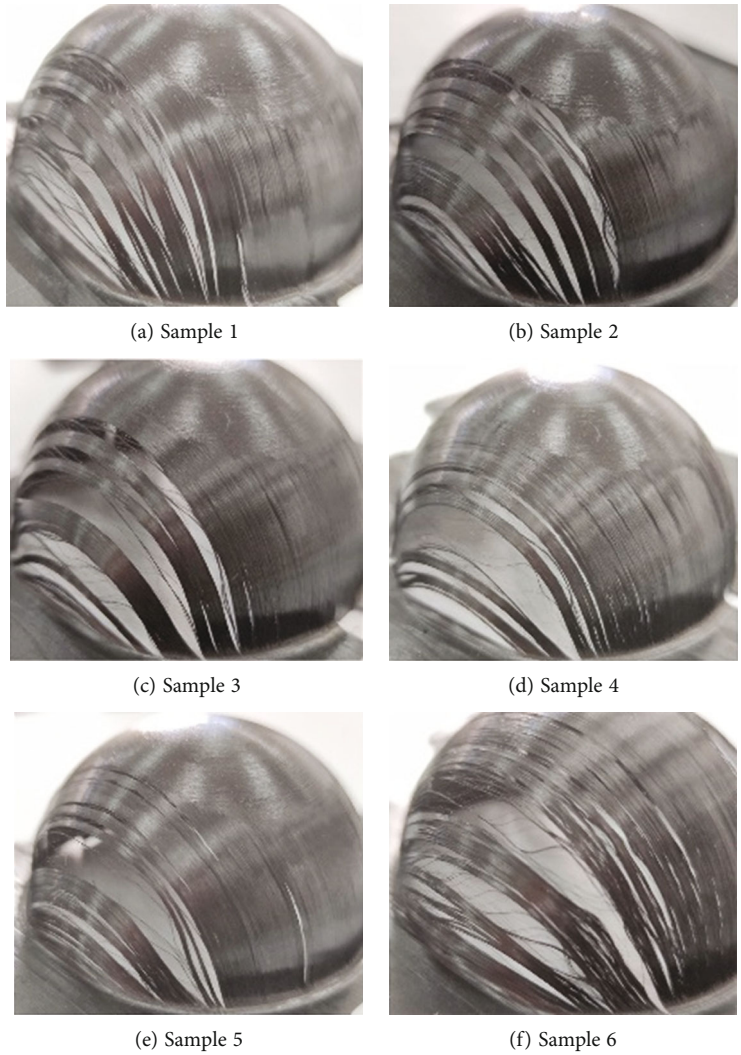

(a) Sample 1 (b) Sample 2

(c) Sample 3 (d) Sample 4

(e) Sample 5 (f) Sample 6

Figure 6: Experimental results of hemispherical molding for single-ply UN-CFRP.

When the bending round corners, due to the anisotropy of UN-CFRP, the bending quality at different bending positions varies greatly under the influence of the fiber angle. By comparing the test results (Figure 6) and finite element simulation results, it is found that the deformation law of the round corner part of the bending is influenced by the angle between the fiber direction and the tangent line of the bending circle (Figure 7). When the deformation zone is located in zone I, the angle between the fiber direction and the tangent line of the round bend is within the range of 60-90° (approximately vertical), the fiber bend is neatly arranged, and the bending quality is good (Figure 8). When the deformation zone is located in the II zone, the fiber direction and circular bending tangent angle are between 15 and 60° range, the fiber by the oblique extrusion pressure will occur at the bend of the oblique extrusion wrinkle, and bending quality is poor (Figure 9). When the deformation zone is located in zone III, the fiber direction and the tangential angle of the circular bend are located in the range of 0-15° (approximately parallel), the fiber by the action of

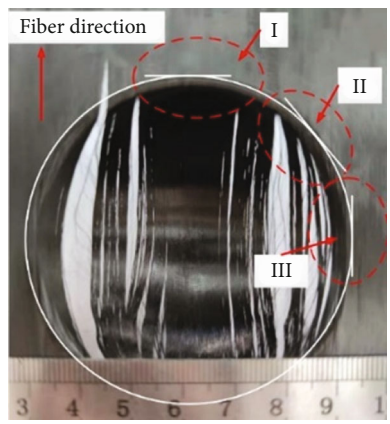

Figure 7: Division of bending areas.

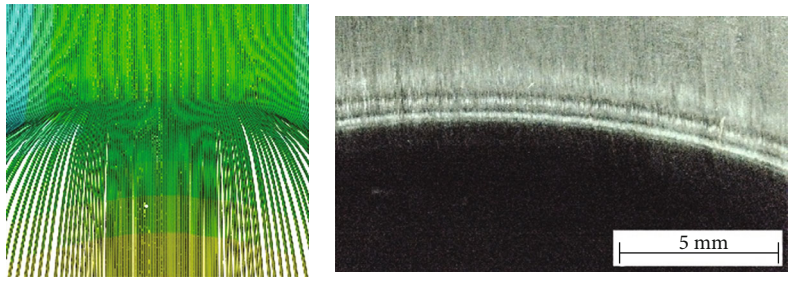

(a) Simulation results (b) Experiment results

Figure 8: Comparison of experimental and simulation results in zone I.

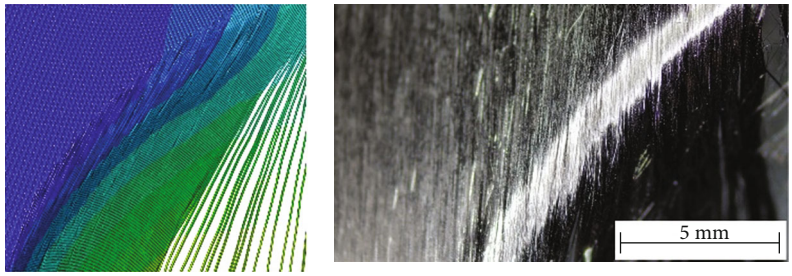

(a) Simulation results (b) Experiment results

Figure 9: Comparison of experimental and simulation results in zone II.

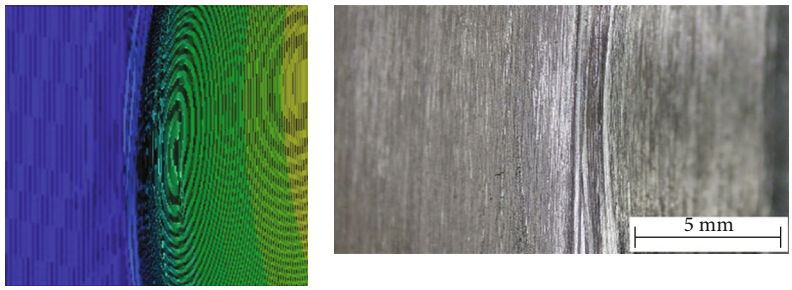

(a) Simulation results (b) Experiment results

Figure 10: Comparison of experimental and simulation results in zone III.

the perpendicular fiber direction of the squeezing pressure will produce extrusion pile-up at the bend, and the bending quality is poor (Figure 10).

4.2. Experimental Results of [0/90] Layered UN-CFRP. From the experimental and simulation analysis results of single-layer UN-CFRP, it can be seen that due to the unidirectional and multiphase nature of UN-CFRP, defects such as dispersion, splitting, and accumulation at corners inevitably occur when performing hemispherical molding experiments, and the full layup of fibers is poor, so in this study, molding experiments were conducted on UN-CFRP with double-layer cross-intersecting layups, and the experimental results are as follows.

Figure 11 shows the experimental results of [0/90] ply UN-CFRP hemispherical molded outer surface; from Figure 11(a), it can be seen that there is no obvious delamination and tear damage on the surface of the specimen under this ply method, and the full spread of the specimen is good. The D and E areas are the intersection of 0° and 90° fibers at the external bend of the hemisphere.

The experimental results show that on the outer surface of the hemisphere, the fiber distribution in zone E (at the corner where the fiber direction is perpendicular to the direction of the circular tangent line at the corner) is of good quality for uniform molding (Figure 11(b)); in zone D (at the corner where the fiber direction is parallel to the direction of the circular tangent line at the corner), the fiber splitting phenomenon is more serious and the fiber distribution quality is poor (Figures 11(c) and 11(d)).

Figure 12 shows the experimental results of the inner surface of the UN-CFRP hemispherical molding for [0/90] layup, from which it can be seen that the specimen has better

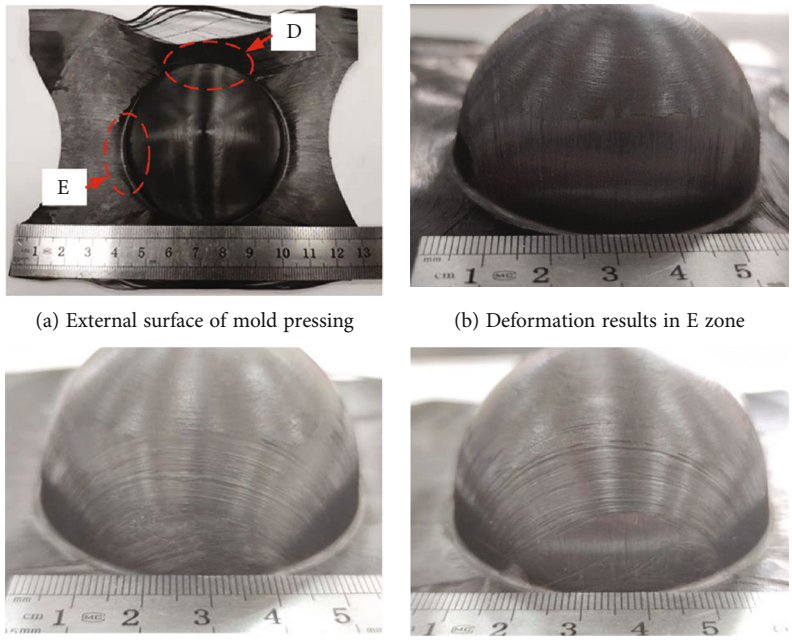

(a) External surface of mold pressing

(b) Deformation results in E zone

(c) Deformation results in D zone

(d) Deformation results in D zone

Figure 11: Experimental results of hemispherical external surface for cross-ply UN-CFRP.

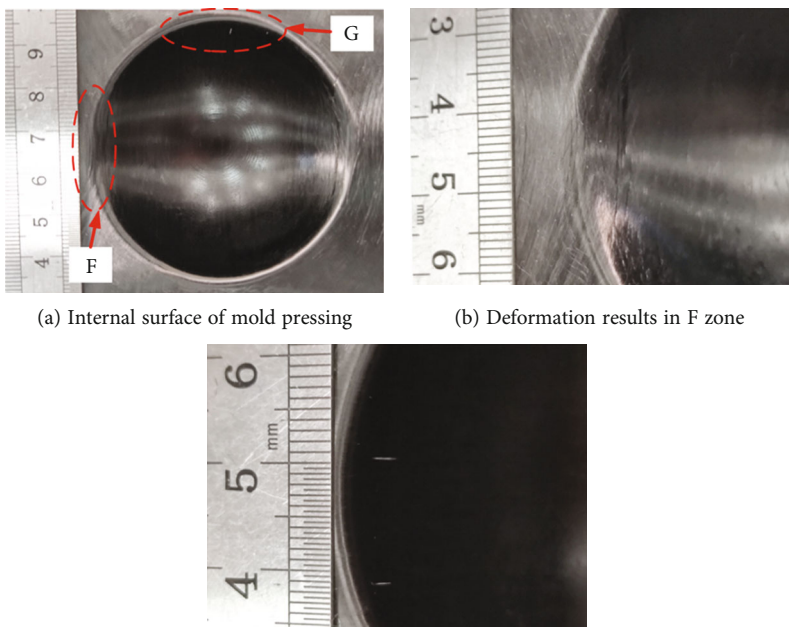

(a) Internal surface of mold pressing

(b) Deformation results in F zone

(c) Deformation results in G zone

Figure 12: Experimental results of hemispherical inner surface for cross-ply UN-CFRP.

full layup and better molding quality. The G and F zones in the figure are the intersection of 0° and 90° fibers at the internal bend of the hemisphere. Theoretically, the results of G and F zones are similar to those of D and E zones, but it is found through the experimental results that the molded quality of the internal part of the hemisphere is higher than that of the external part. Figure 12(b) shows the fiber distribution at the inner surface of the hemisphere, where the fiber direction is parallel to the direction of the circular tangent at the corner, from which it can be seen that the molded quality at this place is higher than that at the outer surface of the hemisphere due to Figures 11(c) and 11(d); Figure 12(c) shows the fiber distribution at the inner surface of the hemisphere, where the fiber direction is perpendicular to the

direction of the circular tangent at the corner, from which it can be seen that there are only a few cracks at this place, and its molded quality is higher than that at the outer surface of the hemisphere due to Figure 11(b) surface. The reason for this difference is analyzed to be due to the gap between the convex and concave die, which leads to the compression of the fiber layer in contact with the convex die and the tension of the fiber layer in contact with the concave die, resulting in the difference in the fiber distribution on the inner and outer surfaces of the specimen. It is noteworthy that no significant folds occur at the internal bend of the specimen when the [0/90] layup UN-CFRP is subjected to hemispherical molding.

5. Analysis of Results

For the molding performance of UN-CFRP, hemispherical molding tests and 3D finite element simulation model were conducted to obtain the deformation law and molding defects of UN-CFRP hemispherical molding. The main conclusions are as follows.

(1) The established hemispherical molding finite element model can accurately predict the deformation pattern and molding defects of UN-CFRP during molding, which proves the validity of the finite element model

(2) When UN-CFRP is molded, the bottom two sides of the specimen in parallel fiber direction show gradient splitting with large splitting amplitude, and the molding quality is poor; the top two sides of the specimen in parallel fiber direction show fan-like dispersion; the top of the specimen in parallel fiber direction is tightly arranged when molded, and the molding quality is good

(3) The angle between the fiber direction and the tangent line at the bend is the main factor affecting the bending quality of UN-CFRP. When the fiber direction and bending tangent angle are located in the range of 70-90°, bending quality is better; when the fiber direction and bending tangent angle are 15-70°, between the range of easy to produce extrusion wrinkles; and when the fiber direction and bending tangent angle are located in the range of 0-15°, easy to produce extrusion pile up

(4) The hemispherical molded specimens with [0/90] layup UN-CFRP have a good molded full layup, but the splitting phenomenon still exists on both sides of the bottom of the specimen in a parallel fiber direction. It is noteworthy that no significant folds occur at the internal bends of the specimens

Data Availability

All data generated or mentioned during this study are included in this published article.

Conflicts of Interest

The authors declare that they have no conflicts of interest.

Acknowledgments

The authors gratefully acknowledge financial support from the Fundamental Research Funds for "Henan province education department natural science research item" (20A460001) and "Start up fund project for high-level talent scientific research of Henan University of Technology" (2020BS051).

References

[1] K. Shaker, Y. Nawab, and A. Saouab, "Experimental and numerical investigation of reduction in shape distortion for angled composite parts," *International Journal of Material Forming*, vol. 13, no. 6, pp. 897–906, 2020.

[2] I. Derbali, S. Terekhina, L. Guillaumat, and P. Ouagne, "Rapid manufacturing of woven comingled flax/polypropylene composite structures," *International Journal of Material Forming*, vol. 12, no. 6, pp. 927–942, 2019.

[3] M. Thor, U. Mandel, M. Nagler et al., "Numerical and experimental investigation of out-of-plane fiber waviness on the mechanical properties of composite materials," *International Journal of Material Forming*, vol. 14, no. 1, pp. 19–37, 2021.

[4] A. Aridhi, M. Arfaoui, T. Mabrouki et al., "Textile composite structural analysis taking into account the forming process," *Composites Part B Engineering*, vol. 166, pp. 773–784, 2019.

[5] M. D. Wakeman, L. Zingraff, P. E. Bourban, J. A. Månson, and P. Blanchard, "Stamp forming of carbon fibre/PA12 composites - a comparison of a reactive impregnation process and a commingled yarn system," *Composites Science and Technology*, vol. 66, no. 1, pp. 19–35, 2006.

[6] B. Alcock, N. O. Cabrera, N. M. Barkoula, and T. Peijs, "Direct forming of all-polypropylene composites products from fabrics made of co-extruded tapes," *Applied Composite Materials*, vol. 16, no. 2, pp. 117–134, 2009.

[7] T. Gereke, O. Döbrich, M. Hübner, and C. Cherif, "Experimental and computational composite textile reinforcement forming: a review," *Compos Part A-Appl S*, vol. 46, no. 46, pp. 1–10, 2013.

[8] P. Harrison, R. Gomes, and N. Curado-Correia, "Press forming a 0/90 cross-ply advanced thermoplastic composite using the double-dome benchmark geometry," *Composites Part A: Applied Science and Manufacturing*, vol. 54, pp. 56–69, 2013.

[9] Q. Zhang, Q. Gao, and S. Zhao, "Thermostamping experimental study on carbon fiber composite sheet," *Journal of Mechanical Engineering*, vol. 48, no. 18, pp. 72–77, 2012.

[10] A. Gherissi, F. Abbassi, A. Ammar, and A. Zghal, "Numerical and experimental investigations on deep drawing of G1151 carbon fiber woven composites," *Applied Composite Materials*, vol. 23, no. 3, pp. 461–476, 2016.

[11] L. Hongfu, Y. Ruijuan, W. Huiping, W. Yang, and Z. Boming, "Preparation of continuous carbon fiber/polyamide 6 prepreg and rectangular box forming by hot stamping," *Acta Materiae Compositae Sinica*, vol. 36, no. 1, pp. 51–59, 2019.

[12] K. Bilisik, "Properties of yarn pull-out in para-aramid fabric structure and analysis by statistical model," *Compos Part A-Appl S*, vol. 42, no. 12, pp. 1930–1942, 2011.

[13] A. Charmetant, E. Vidal-salle, and P. Boisse, "Hyperelastic modelling for mesoscopic analyses of composite reinforcements," *Composites Science and Technology*, vol. 71, no. 14, pp. 1623–1631, 2011.

[14] S. Davey, R. Das, W. J. Cantwell, and S. Kalyanasundaram, "Forming studies of carbon fibre composite sheets in dome forming processes," *Composite Structures*, vol. 97, pp. 310–316, 2013.

[15] Q. Zhang, Q. Gao, and J. Cai, "Experimental and simulation research on thermal stamping of carbon fiber composite sheet," *Transactions of the Nonferrous Metals Society of China*, vol. 24, no. 1, pp. 217–223, 2014.

[16] Y. Gong, X. Peng, Y. Yao, and Z. Guo, "An anisotropic hyperelastic constitutive model for thermoplastic woven composite prepregs," *Composites Science and Technology*, vol. 128, no. - May 18, pp. 17–24, 2016.

[17] X. Q. Peng and J. Cao, "A continuum mechanics-based non-orthogonal constitutive model for woven composite fabrics," *Compos Part A-Appl S*, vol. 36, no. 6, pp. 859–874, 2005.

[18] S. P. Haanappel, R. H. W. Ten Thije, U. Sachs, B. Rietman, and R. Akkerman, "Formability analyses of uni-directional and textile reinforced thermoplastics," *Compos Part A-Appl S*, vol. 56, pp. 80–92, 2014.

[19] P. Badel and B. P. Vidal-salle, "Computational determination of in-plane shear mechanical behaviour of textile composite reinforcements," *Computational Materials Science*, vol. 40, no. 4, pp. 439–448, 2007.

[20] P. Boisse, B. Zouari, and A. Gaaaer, "A mesoscopic approach for the simulation of woven fibre composite forming," *Composites Science and Technology*, vol. 65, no. 3–4, pp. 429–436, 2005.

[21] H. Wang, X. Zhang, and Y. Duan, "Effects of drilling area temperature on drilling of carbon fiber reinforced polymer composites due to temperature-dependent properties," *International Journal of Advanced Manufacturing Technology*, vol. 96, no. 5-8, pp. 2943–2951, 2018.

[22] P. Boisse, N. Hamila, E. Vidal-Sallé, and F. Dumont, "Simulation of wrinkling during textile composite reinforcement forming. Influence of tensile, in-plane shear and bending stiffnesses," *Composites Science and Technology*, vol. 71, no. 5, pp. 683–692, 2011.